

A New Type of Noble Metal Mineralization in Terrigenous Rocks of the Shatak Graben, Western Slope of the Southern Urals

S. G. Kovalev^a and I. V. Vysotskii^b

^a*Institute of Geology, Ufa Scientific Center, Russian Academy of Sciences,
ul. Karla Marksa 16/2, Ufa, 450000 Russia
e-mail: kovalev@anrb.ru*

^b*Bashgeoltsentr State Unitary Association, ul. Lenina 37, Ufa, Bashkortostan, 450077 Russia
Received July 4, 2005*

Abstract—The paper presents materials on a new (unconventional for the Urals) noble metal (platinum–gold–iron oxide) mineralization confined to terrigenous sequences of the Middle Riphean Mashak Formation on the western slope of the southern Urals. The mineralization is related to the percolation of reduced mantle fluids into upper levels of the crust at early stages of riftogenesis, their inversion in the crust, and redeposition of ore-forming elements.

DOI: 10.1134/S0024490206040079

The Shatak graben, an element of the Middle Riphean paleorift, is located in the southern part of the eastern limb of the Yamantau anticlinorium within the Bashkirian meganticlinorium (Fig. 1). The graben is composed of terrigenous, magmatic, and volcanosedimentary rocks of the Middle Riphean (R_2) Mashak Formation. In terms of the lithology and bedding succession, the Mashak Formation is divided into eight subformations. The first and sixth subformations are volcanosedimentary units. The second and fourth subformations are volcanic-rich units. The third, fifth, seventh, and eighth subformations are terrigenous units (Rotar et al., 1982). The terrigenous rocks (~75 vol % of the Mashak Formation) are mainly composed of coarse-grained rocks (quartz–quartzite sandstones and conglomerates) with subordinate siltstones and carbonaceous shales. Conglomerate units (thickness up to 20–25 m, length up to 10–12 km) are widespread in the Kuz’elga (R_{2ms_1}), Kuyantav (R_{2ms_5}), and Karan (R_{2ms_6}) subformations. The conglomerates are represented by all varieties ranging from the fine- and coarse-pebble rocks. The clastic material is composed of well rounded pebbles and boulders of quartzite sandstone, quartzite, and less common quartz. The quartz–sericite, quartz–sericite–chlorite, and less common quartz–epidote–chlorite matrix includes a significant amount of magnetite and hematite associated with traces of sulfides.

Basic and acid volcanics of the Mashak Formation are represented by the sheet (effusive and pyroclastic) and subvolcanic (sills and dikes) facies. In addition, the formation base includes a differentiated diabase–picrite body that represents the first portion of an undifferentiated mantle melt formed at the early stage of rift formation (Kovalev and Vysotskii, 2003).

The comprehensive examination of terrigenous sequences (primarily, conglomerates of the Kuz’elga and Karan subformations) in recent years yielded original data on their metal potential and made it possible to recognize a new type of noble metal mineralization in the Urals.

COMPOSITION AND STRUCTURE OF ROCKS

Kuz’elga Subformation

The Kuz’elga Subformation is developed on the western slope of the Bol’shoi Shatak Ridge as a submeridional band from 300 to 700 m wide and more than 11 km long. The internal structure of the subformation is characterized by alternation of conglomerates and sandstones in the lower part (85–100 m), conglomerates and diabases in the middle part (130–140 m), and rhyolites in the upper part (up to 180 m).

The summary geological section of the Kuz’elga Subformation is as follows (from bottom to top):

(1) Alternation of carbonaceous quartz–sericite–chlorite and chlorite–sericite schists, siltstones, and quartzite-type sandstones of the Lower Riphean Yusha Formation. At the contact with the overlying Kuz’elga Subformation, the rocks are bleached and marked by abundant chloritoid dissemination.

In the central Shatak graben, contact zone between the Yusha and Mashak subformations incorporates a layered 20-m-thick and 3-km-long diabase–picrite pluton that can be divided into three zones.

The lower zone is composed of picrodiabases intensely altered by secondary processes. Primary clinopyroxene is inferred from pseudomorphoses. The presence of plagioclase is problematic (vague plagioclase

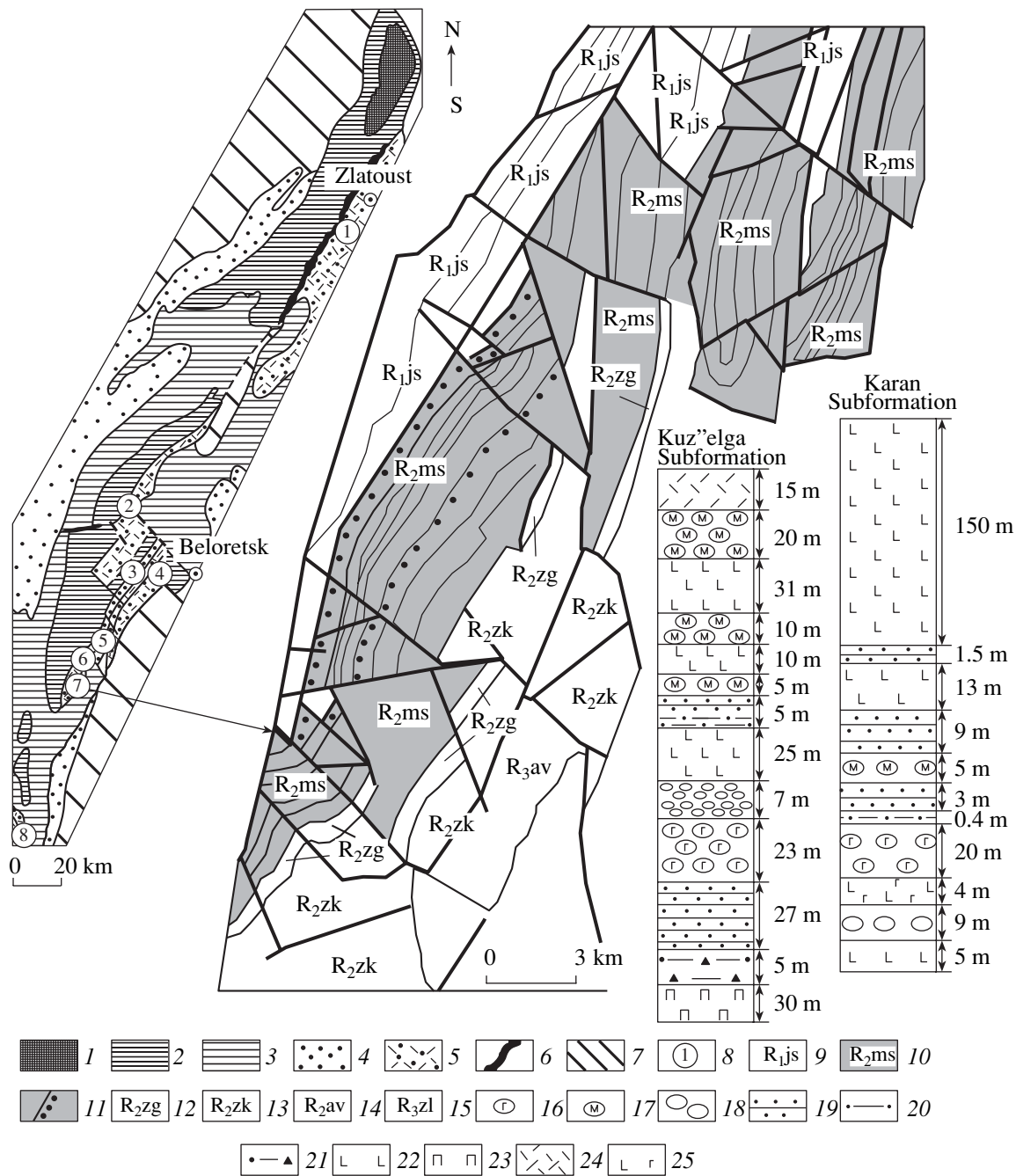


Fig. 1. Geological scheme of the western slope of the southern Urals and lithological sections of the Mashak Formation. (1) Archean–Proterozoic Taratash Complex; (2) Lower Riphean rocks; (3) Middle Riphean sedimentary rocks; (4) Upper Riphean–Vendian rocks (undifferentiated); (5) Middle Riphean volcanosedimentary rocks; (6) Kusa–Kopan intrusive complex; (7) Paleozoic rocks (undifferentiated); (8) lithostructural complexes of the Middle Riphean paleorift (numbers in circles): (1) Kuvash, (2) Mashak, (3) Ishlin, (4) Beletar, (5) Uzyan, (6) Kukhtur, (7) Shatak, (8) Kurgas; (9) Yusha Formation (R₁), (10) Mashak Formation (R₂); (11) conglomerate units; (12) Zigal'ga Formation (R₂); (13) Zigaza–Komarovo Formation (R₂); (14) Avzyan Formation (R₂); (15) Zil'merdak Formation (R₃); (16) conglomerate with hematite; (17) conglomerate with magnetite; (18) gritstones; (19) sandstones; (20) silty sandstones; (21) tectonic breccia; (22) metabasalts; (23) differentiated diabase–picrite intrusion; (24) rhyolites; (25) hematized basic rocks.

clase plates replaced by secondary minerals are subordinate). Secondary minerals are represented by amphibole, sphene, leucoxene, chlorite, serpentine, albite, carbonate, apatite, talc, and sericite. The

amphibole commonly occurs as colorless tremolite, but greenish actinolite crystallites are also found. Some minerals are locally replaced by albite and serpentine. Ore mineral is represented by skeletal leucoxenized

titanite segregations, probably, developed after the primary titanomagnetite. The rock also contains chalcopyrite (up to 2–5%) and anhedral segregations of red spinel (probably, picotite).

The central zone of the pluton is composed of picrites. Primary minerals in these rocks are represented by olivine, clinopyroxene, orthopyroxene, and hornblende. Secondary minerals are represented by amphibole, talc, chlorite, epidote, serpentine, muscovite (sericite), magnetite, titanite, and apatite. The rocks are intensely altered and almost completely transformed into a talc–amphibole–serpentine aggregate. Amphibole is represented by tremolite, while actinolite is less common. The presence of orthopyroxene is inferred from solitary bastite pseudomorphoses. Magnetite occurs as subhedral and euhedral dissemination. Titanite is developed as irregular grains. The central unit is characterized by pseudolayered (banded) structure related to the alternation of cumulative pseudolayers enriched in olivine and pyroxene.

The upper (near-contact) zone consists of metadiabases with the microdiabase and microdolerite textures. The rocks are composed of pyroxene, plagioclase, magnetite, chlorite, sphene, epidote, actinolite, apatite, and albite. The euhedral plagioclase laths make up felted aggregates in some places. Pyroxene is completely replaced by chlorite (pennine) and acicular actinolite. Epidote makes up granular patches and stringers. Magnetite (8–10%) occurs as subhedral and anhedral segregations often associated with fine-grained aggregates of the leucoxenized titanite.

The outer contact zone of the differentiated pluton includes tectonic breccia (chloritized silty sandstones with gruss and rubble of bleached schists).

(2) Pinky gray thick-platy quartzite-type sandstones grading from medium-grained rocks in the lower part to coarse-grained sandstones in the upper part and gritstones at the top. The clastic material is mainly composed of quartz, while quartzites, microquartzites, and schists are less common. The matrix is composed of quartz–sericite and chlorite–sericite aggregates. The content of ore mineral (hematite) is as much as 10–15%. The rocks contain abundant dissemination of secondary chloritoid.

(3) Coarse-pebble and boulder conglomerates (with 70–80% of boulder–pebble material) in the lower part and fine-pebble conglomerates in the upper part. They grade into gritstones and coarse-grained sandstones. The boulders and pebbles consist of quartzites (in places, quartz). The matrix is composed of the quartz–sericite–chlorite aggregate. Like in the underlying sandstones, ore mineral is mainly represented by hematite. Pyrite is insignificant (<1%).

(4) Columnar greenish gray diabases with massive structure and microdolerite and microdiabase textures. The rocks are composed of chlorite, epidote, actinolite, titanite, prehnite, and quartz.

(5) Greenish gray thin-platy siltstones composed of quartz (<0.01 mm) and the sericite–chlorite matrix.

(6) Boulder–pebble conglomerates with the quartz–sericite–chlorite and epidote–chlorite matrix. Ore mineral is represented by euhedral magnetite crystals. Tiny (micrometer-scale) pyrite inclusions are present in the magnetite and nonore minerals. The contact zone with the underlying diabases includes chalcopyrite (up to 2–3%), subordinate pyrrhotite, and rare native iron represented by gray segregations with metallic luster and irregular vermicular shape (up to 2–3 mm long). The microprobe analysis showed that the native iron has the following composition (at %): Fe 97.62–99.33; Mn 0.54; Au 0.30–0.33; Pt 0.4, and Cr 0.34–1.14 (Kovalev and Vysotskii, 2000).

(7) Columnar diabases represented by schistosed and chloritized rocks in the lower part, massive rocks in the middle part, and amygdaloidal varieties at the top.

(8) Boulder–pebble conglomerates (boulders up to 25–30 cm in size) composed of quartzites and less common quartz. The matrix is composed of quartz–sericite–chlorite and epidote–chlorite aggregates. Magnetite is the major ore mineral.

(9) Greenish gray diabases represented by schistosed and ferruginated rocks in the lower part. In the middle and upper parts, the rocks are represented by massive varieties with amygdules filled with copper hydroxides, quartz, and epidote.

(10) Violet platy siltstones with euhedral magnetite crystals (up to 10–15%).

(11) Boulder–pebble conglomerates with chloritized quartzite clasts. The matrix is composed of the fine-grained quartz–chlorite–sericite aggregate with secondary acicular zoisite segregations and granular epidote. Euhedral magnetite crystals are developed in both the matrix and pebbles.

(12) Porphyritic rhyolites and rhyodacites with microlitic texture of the groundmass and multidirectional structure. The porphyritic segregations are represented by the sericitized feldspar. The groundmass is replaced by quartz micrograins and has feldspar–quartz composition with an admixture of chloritized and epidotized biotite. The ore mineral is represented by subhedral “melted” magnetite crystals up to 1 mm in size (3–5%).

Based on mineral assemblages of sedimentary rocks and type of ore mineralization, one can divide the Kuz’elga Subformation into the lower and upper sequences. The lower sequence is characterized by the regressive–transgressive section with thickness varying from 80 to 100 m at different exposures. Hematite, the major ore mineral in these rocks, is developed in both the conglomerate matrix and pebbles. The X-ray phase analysis showed that the hematite-bearing conglomerate matrix is composed of quartz (92–95%), biotite and muscovite (up to 10%), magnetite (~1%), and hematite (10–15%). The lower part contains abundant chloritoids (up to 10–15%).

Table 1. Contents of noble metals in sedimentary and magmatic rocks of the Shatak Complex, g/t

Rock	Au	Ag	Pt	Pd
Conglomerate with magnetite	0.20	5.25	1.75	0.30
Sandstone with hematite	0.25	1.00	<0.5	<0.1
Diabase with magnetite	<0.1	1.75	<0.5	<0.1
Conglomerate with sulfides	0.10	1.00	<0.5	<0.1
Conglomerate	0.35	1.25	n.d.	n.d.
Conglomerate with hematite	1.80	1.45	n.d.	n.d.
Conglomerate with magnetite	1.60	2.50	1.30	0.30
Conglomerate with magnetite	1.20	1.00	1.50	0.20
Magnetite ore	1.20	1.75	<0.5	<0.1
Conglomerate with magnetite	2.15	1.20	1.40	0.20
Conglomerate	0.20	1.38	n.d.	n.d.
Conglomerate	0.30	1.25	<0.5	<0.1
Carbonaceous shale with sulfides	0.20	1.36	<0.5	<0.1
Conglomerate	<0.1	1.00	<0.5	<0.1
Conglomerate	0.20	1.25	<0.5	<0.1
Conglomerate	0.20	1.00	n.d.	n.d.
Conglomerate	0.15	0.75	n.d.	n.d.
Conglomerate	0.20	0.75	0.85	0.20
Conglomerate	0.20	0.75	0.60	0.20
Conglomerate	1.80	1.40	1.25	0.35
Conglomerate	1.60	2.55	1.30	0.30
Conglomerate with hematite	1.85	1.70	0.50	0.10
Gritstone with hematite	0.20	0.50	<0.5	<0.1
Conglomerate	0.10	0.50	n.d.	n.d.
Sandstone with hematite	0.20	1.25	n.d.	n.d.
Conglomerate	2.00	0.75	0.80	0.30
Conglomerate	0.10	1.00	n.d.	n.d.
Conglomerate	0.10	0.50	n.d.	n.d.
Diabase with magnetite	<0.1	1.75	<0.5	<0.1
Carbonaceous shale	0.20	1.38	n.d.	n.d.

Note: Analyses were carried out by the atomic absorption method at the Unipromed Open Joint-Stock Association. (n.d.) Not determined.

The atomic absorption analysis showed that hematite fractions taken from the conglomerate matrix in the lower sequence of the Kuz'elga Subformation contains Au (up to 10.77 g/t) and Ag (1.12 g/t). In addition to Fe (8.22 wt %), the bulk samples contain the following noble metals (g/t): Au 1.8, Ag 1.4, Pt up to 1.25, and Pd up to 0.35 (Table 1).

The upper sequence can be divided into three units of boulder-pebble conglomerates with a total thickness of ~50 m. They alternate with diabase flows (sills) overlapped by rhyolites in the upper part of the section. The

conglomerate matrix is characterized by the presence of secondary minerals of the epidote-zoisite group associated with chlorite. Euhedral magnetite crystals (0.5–2 mm) are found in both the matrix and pebbles. The magnetite fraction contains Au (up to 4.9 g/t) and Ag (0.2 g/t). The maximal content of noble metals in bulk samples is as follows (g/t): Pt 1.75, Pd 0.30, Au 2.15, and Ag 5.25. The Fe content is 6.54 wt %.

High contents of noble metals are consistent with the microprobe detection of iron oxyhydroxides in these rocks (Table 2).

Karan Subformation

In terms of lithology and petrography, the Karan Subformation is similar to the Kuz'elga Subformation. Rocks of the Karan Subformation make up a rather persistent submeridional band on the eastern slope of the Bol'shoi Shatak Ridge. The summary section of the Karan Subformation is as follows (from bottom to top):

(1) Greenish gray diabases represented by massive and aphyric rocks in the middle part and by amygdaloidal and brecciated varieties at the top.

(2) Boulder-pebble conglomerates with quartzitic sandstone clasts up to 20 cm in size. The matrix (15% of the groundmass) has a polymictic composition.

(3) Intensely schistosed, chloritized, and hematitized basic rocks (metadiabases) characterized by separation into boudins and dissemination of fine euhedral magnetite crystals (up to 20–25%).

(4) Boulder-pebble conglomerates with the hematitized quartz-sericite-chlorite matrix.

(5) Dark gray schistosed siltstones.

(6) Varigrained greenish gray thick-platy schistosed sandstones.

(7) Boulder-pebble conglomerates similar to unit 4. In the southern part of the Shatak graben, the conglomerates overlie metadiabases of unit 3. In the contact zone, both diabases and conglomerates contain abundant magnetite dissemination (up to 60–70%). Thus, the rocks actually represent magnetite ore.

(8) Sandstones represented by medium-grained rocks in the lower and middle parts. At the top, the rocks are represented by massive quartzite-type rocks with pentagon dodecahedral pyrite inclusions (up to 5%).

(9) Diabases represented by epidotized rocks at the bottom and silicified brecciated varieties (with 5–7% of fine magnetite dissemination) at the top.

(10) Sandstones represented by coarse-grained rocks at the bottom and quartzitic sandstones (with thin quartz veinlets) at the top.

(11) Greenish gray diabases. The rocks are replaced by amphibolites at the lower outer contact. In the middle part, they are represented by epidotized rocks containing S-shaped (ladder-type) quartz veinlets and

Table 2. Chemical composition of magnetite in rocks of the Shatak Complex (at %)

Element	1	2	3	4	5	6	7
Au	0.0	0.0	0.0	0.0	0.225	0.508	0.0
Ag	0.67	0.0	0.0	0.0	0.106	0.0	0.112
Pt	0.0	0.0	0.0	0.0	0.0	0.518	0.344
Pd	0.484	0.0	0.234	0.0	0.038	0.0	0.685
Rh	0.143	0.0	0.0	0.0	0.0	0.148	0.203
Fe	97.123	98.96	97.296	98.705	98.423	97.365	96.021
S	0.0	0.088	0.823	0.064	0.094	0.0	0.0
Cr	0.104	0.085	0.161	0.285	0.133	0.0	0.0
Co	0.0	0.0	0.0	0.0	0.0	0.233	0.0
Ni	0.157	0.151	0.189	0.195	0.0	0.143	0.403
Cu	0.063	0.048	0.153	0.168	0.087	0.0	0.362
Ti	0.068	0.068	0.077	0.479	0.073	0.238	0.178
V	0.554	0.014	0.205	0.0	0.078	0.374	0.095
Sn	0.0	0.0	0.0	0.104	0.184	0.0	0.0
Mn	0.052	0.0	0.0	0.0	0.0	0.149	0.326
Sb	0.107	0.213	0.0	0.0	0.094	0.0	0.0
As	0.475	0.373	0.0	0.0	0.0	0.092	1.271
Pb	0.0	0.0	0.862	0.0	0.465	0.232	0.0

Note: (1–5) From conglomerates and gritstones; (6, 7) from diabases. The mineral composition was determined with a JSM-840 scanning microscope equipped with Link (accelerating voltage 20 kV, count time 50 s) at the Institute of Problems of Superplasticity of Metals, Russian Academy of Sciences (Ufa). Pure metals were used as standards.

quartz–epidote veins with chalcopyrite and copper hydroxide.

In terms of the major ore mineral assemblage, the Karan conglomerate, like the Kuz'elga conglomer-

ate, can be divided into the hematite and magnetite varieties. In the first variety, the hematite content varies from a few grains (conglomerate pebbles) to 15–20% (conglomerate matrix). Magnetite is devel-

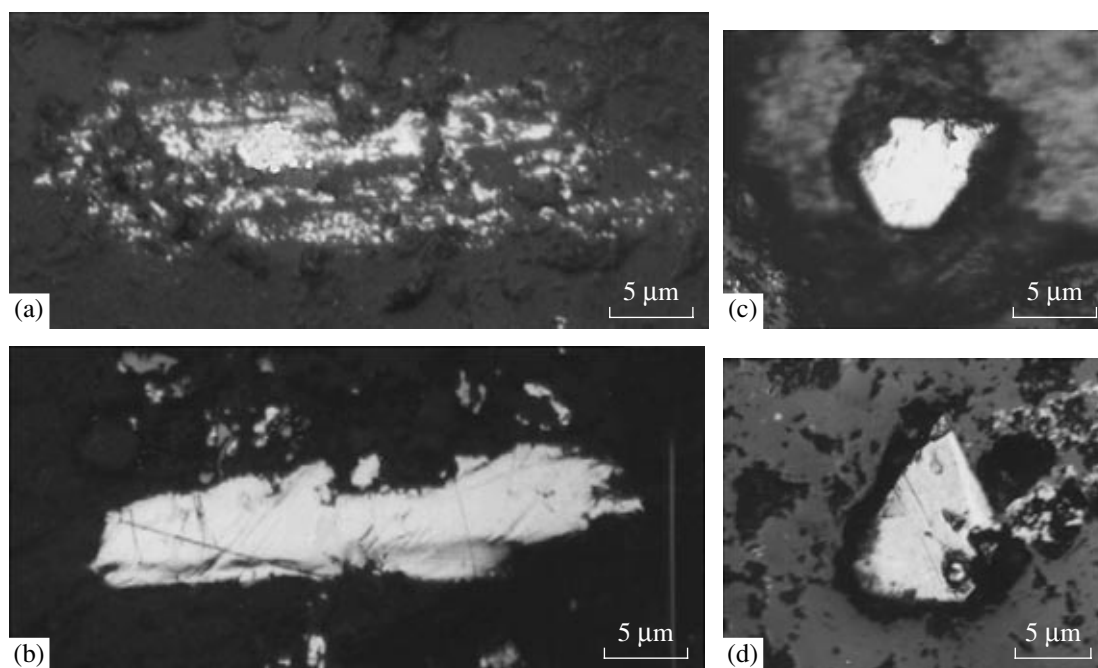


Fig. 2. (a, b) Native gold and (c, d) platinum group metals in Shatak conglomerates.

oped as a sporadic mineral (primarily, in association with hematite) in the quartz matrix. It occurs as euhedral crystals (30–150 μm) with well-developed three to six faces.

Magnetite makes up nonuniform dissemination (60–65%) in the magnetite-bearing conglomerate. The magnetite is often replaced by iron oxyhydroxides. For example, the base of a triangular crystal detected in one polished sample is composed of magnetite overgrown with a thin hematite plate (30–40 μm). The apex is composed of lepidocrocite.

Both types of conglomerate contain native gold inclusions primarily confined to the chlorite–ferruginous segregations that cement the quartz grains. The gold grains occur as irregular (with zigzag edges), dendritic, and drop-shaped particles. Their size is generally 1–5 μm , but one can also see larger grains (Figs. 2a, 2b). In addition, optical study in the Mineralogical laboratory of the Unipromed Open Joint-Stock Association revealed niggliite (PtSn_3) in two samples. The mineral is characterized by euhedral shape with two or three smooth faces (Figs. 2c, 2d), medium hardness, very strong birefringence ($R = 20\text{--}40\%$), and distinct anisotropy ranging from the orange to dark grayish blue color.

DISCUSSION

It is believed at present that the terminal Early Riphean–initial Middle Riphean boundary on the western slope of the southern Urals represents the initial epoch of riftogenic structure formation (Parnachev et al., 1986; Ivanov et al., 1989; Kovalev, 2004). This period marked the origination of several graben-shaped structures filled with psephitic–psammitic sediments of the Mashak Formation. Reactivation of magmatic processes is reflected in the formation of igneous rocks with different Ca contents (from microbasalts to rhyolites) and facies affiliations (effusive flows, subvolcanic stratabound bodies, and eruptive neck complexes). The injection of large volumes of basaltic magma into upper levels of the Earth's crust is always accompanied by the preliminary processing of the substrate by mantle-derived reduced fluids that are separated from the melt at a depth of ~10 km (Zotov, 1989). This is preceded by concentration of ore-forming elements in the upper part of the fluid-magmatic column. Injection of fluids into upper levels of the Earth's crust along the tectonically weakened zones provokes changes in redox conditions, leading to the formation of mantle-related geochemical anomalies of elements. Concentration of ores in the course of the subsequent evolution is promoted not only by lithostructural features, but also the duration of functioning of fluid-hydrothermal sources.

We substantiate physicochemical constraints of the platinum–gold–iron mineralization on the basis of (Marakushev and Bezmen, 1971), according to which

growth of the positive free energy of reactions of the $\text{MeO}_2 + \text{S}_2 = \text{MeS}_2 + \text{O}_2$ type with increase in temperature indicates the progressive shift of reaction equilibrium to the left side (i.e., toward the formation of oxides). This is consistent with the empirical trend, according to which the replacement of oxide mineralization by sulfide type in ore deposits is accompanied by decrease in temperature. Calculations of equilibrium relations between magnetite and iron sulfides in systems with the participation of HS^- and OH^- revealed that magnetite is more stable than iron sulfides at $>400^\circ\text{C}$. Decrease in temperature below 400°C fosters the appearance of the pyrite–pyrrhotite assemblage instead of magnetite (Pavlov, 1976).

Thus, increase in oxygen fugacity, which is reflected in the higher affinity of metals with oxygen, governs the stability of iron oxides and silicates. Under such conditions, gold and platinum demonstrate siderophile properties, promoting their joint migration with Fe. This interpretation is supported by the findings of native gold in the conglomerate matrix. In contrast to Pt, Pd is a typical chalcophile element. Therefore, Pd is atypical for the gold–platinum–iron oxides assemblage. This is reflected in high values of the Pt/Pd ratio (average 4).

CONCLUSIONS

Materials presented in this paper indicate that the gold–platinum–iron oxides assemblage formed in conglomerates of the Mashak Formation from reduced fluids at a temperature of $>400^\circ\text{C}$. The metals were derived from mantle fluids injected into upper levels of the Earth's crust.

ACKNOWLEDGMENT

This work was supported in part by the Earth Science Division of the Russian Academy of Sciences.

REFERENCES

- Ivanov, S.N., Koroteev, V.A., Puchkov, V.N., and Ivanov, K.S., Evolution of Rift Systems in the Urals, in *Tektonicheskie protsessy* (Tectonic Processes), Moscow: Nauka, 1989, pp. 154–163.
- Kovalev, S.G., Formation Dynamics of the Middle Riphean Riftogenic Structure (Western Slope of the Southern Urals), *Dokl. Akad. Nauk*, 2004, vol. 396, no. 2, pp. 219–222 [*Dokl. Earth. Sci.* (Engl. Transl.), 2004, vol. 396, no. 2, pp. 481–487].
- Kovalev, S.G. and Vysotskii, I.V., First Findings of Native Iron in Rocks of the Mashak Complex and Their Petrographic Implications, in *Geologicheskii sbornik. Informatsionnye materialy* (Geological Collection: Information Materials), Ufa: Inst. Geol. Ural. Tsent. Akad. Nauk, 2000, no. 1, pp. 86–87.
- Kovalev, S.G. and Vysotskii, I.V., New Data on Magmatism in the Shatak Graben, in *Geologicheskii sbornik-3. Informa-*

tsionnye materialy (Geological Collection-3. Information Materials), Ufa: Inst. Geol. Ural. Tsentr Akad. Nauk, 2003, no. 3, pp. 117–119.

Marakushev, A.A. and Bezmen, N.I., *Termodinamika sul'fidov i okislov v svyazi s problemami rudoobrazovaniya* (Thermodynamics of Sulfides and Oxides in Connection with Problems of Ore Formation), Moscow: Nauka, 1971.

Parnachev, V.P., Rotar, A.F., and Rotar, Z.M., *Srednerifeiskaya vulkanogenno-osadochnaya assotsiatsiya Bashkirskogo megantiklinoriya (Yuzhnyi Ural)* (Middle Riphean Volcanosedimentary Association in the Bashkirian Meganticlinorium, Southern Urals), Sverdlovsk: Ural. Nauchn. Tsentr Akad. Nauk SSSR, 1986.

Pavlov, A.L., *Evolutsiya fiziko-khimicheskikh parametrov gidrotermal'nykh sistem pri rudoobrazovanii* (Evolution of Physicochemical Parameters of Hydrothermal Systems during Mineralization), Novosibirsk: Nauka, 1976.

Rotar, A.F., Rotar, Z.M., and Parnachev, V.P., Stratigraphy of the Shatak Formation, Middle Riphean in the Southern Urals, in *Stratigrafiya i litologiya dokembriiskikh i rannepaleozoiskikh otlozhenii Urala* (Stratigraphy and Lithology of Precambrian and Early Paleozoic Rocks in the Urals), Sverdlovsk: Inst. Geol. Geokhim. Dokembr., 1982, pp. 53–64.

Zotov, I.A., *Transmagmaticheskie flyuidy v magmatizme i rudoobrazovanii* (Transmagmatic Fluids in Magmatism and Ore Formation), Moscow: Nauka, 1989.